Available online at www.sciencedirect.com
SCIENCE DIRECT®
ELSEVIER
Journal of Magnetism and Magnetic Materials 301 (2006) 94–99
Journal of magnetism and magnetic materials
www.elsevier.com/locate/jmmm

# The optimum grain size for minimizing energy losses in iron

M.F. de Campos[a], J.C. Teixeira[b], F.J.G. Landgraf[b,*]

[a]*Escola de Engenharia Industrial Metalúrgica de Volta Redonda/Universidade Federal Fluminense Av. dos Trabalhadores 420, Vila Santa Cecília, 27255-125, Volta Redonda, RJ, Brasil*
[b]*Instituto de Pesquisas Tecnológicas do Estado de São Paulo, Av. Prof. Almeida Prado 532, 05508-901, São Paulo, SP, Brasil*

Received 12 September 2004; received in revised form 21 June 2005
Available online 18 July 2005

**Abstract**

A model able to predict the optimum grain size for textured electrical steels used in motors or transformers is presented. The model is based on the Pry and Bean model for the anomalous losses. The validity of the model is restricted to the frequency range of 1–1000 Hz. The model predicts that the optimum grain size decreases as: resistivity decreases or frequency increases or thickness of steel sheet increases. The predictions of the model are compared with experimental results.


*PACS:* 75.50.−y; 75.50.Bb; 75.60.−d; 75.60.Ej

*Keywords:* Electrical steels; Iron losses; Hysteresis; Grain size; Texture

## 1. Introduction

Most of the electrical energy produced in the entire world is consumed in electrical motors [1], which are rotating machines that employ non-oriented electrical steels as soft magnetic materials. The high magnetic induction of iron and iron-rich alloys (for pure iron, the magnetic induction is 2.17 T) and their low cost are decisive in the choice of steels for energy conversion purposes, as in the case of electrical motors. Although much recent research has been focused on other possible alternatives for energy storage and energy conversion, there is also an enormous motivation for research on the optimization of electrical steels—as well as on research for improvement of the efficiency of electrical motors—as a feasible method for energy saving.

Although it is well known that there is an optimum grain size for minimizing the iron losses [2–7], the influence of variables such as electrical resistivity and frequency on the optimum grain size is not well known. The present study has the objective of providing a simple mathematical

*Corresponding author. Tel.: +55 11 3767 4211.
*E-mail addresses:* mcampos@metal.eeimvr.uff.br (M.F. de Campos), landgraf@ipt.br (F.J.G. Landgraf).

0304-8853/$ - see front matter © 2005 Elsevier B.V. All rights reserved.
doi:10.1016/j.jmmm.2005.06.014

model of this subject. This work also intends to give guidance in choosing a steel when designing new electrical motors.

## 2. Experimental

The chemical composition of the steel is given in Table 1. The samples (steel sheets with thickness of 0.53 mm) were subjected to a skin-pass (reduction of thickness) of either: 0, 4, 7, 11, 13, or 17%. Later, the samples were annealed at 760 °C [6,7]. This procedure gives rise to a gradual change of the recrystallized grain size, as shown in Table 2.

Grain size ($G_s$) was measured by the intercept method on polished and 2%Nital etched samples. As seen in Table 2, a gradual change of the grain size ($G_s$) was obtained in steel sheets by using a simple metallurgical rule: on increasing the cold-rolling reduction, more energy is stored during the deformation, promoting more frequent nucleation of new grains, and smaller is the recrystallized grain size. Unfortunately, this method also introduces the thickness of the sample as a kind of "second variable". However, this effect can, in principle, be considered negligible except as mentioned below.

Magnetic measurements were done in an Epstein frame, using a system of data acquisition that includes measurements at quasi-static condition (i.e., $f \to 0$). Texture data were acquired in a Philips X-Pert Diffractometer equipped with a texture goniometer using CoK$\alpha$ radiation.

Table 1
Chemical composition and resistivity of the alloy

| %Si | %Al | %Mn | %P | %S | $N$ (ppm) | $\rho$ ($\mu\Omega$ cm) |
|---|---|---|---|---|---|---|
| 0.54 | 0.04 | 0.31 | 0.045 | 0.006 | 53 | 20.5 |

Table 2
Relationship between skin-pass and recrystallized grain size

| Skin-pass (%) | 0 | 17 | 13 | 11 | 7 | 4 |
|---|---|---|---|---|---|---|
| $G_s$ ($\mu$m) | 13 | 48 | 104 | 125 | 163 | 360 |

## 3. Results and discussion

### 3.1. The loss separation procedure

In the power Losses separation procedure [8], the total losses $P_t$ are separated into three components, the classical eddy losses $P_{cl}$, the anomalous or excess losses $P_a$ and hysteresis losses $P_h$ (according to the expression below).

$$P_t = P_h + P_{cl} + P_a. \quad (1)$$

The contribution of eddy currents to energy dissipation can be estimated according to the "classical" expression, as described by Thomson in the XIX Century [9]:

$$P_{cl} = \frac{\pi^2 f^2 B_{max}^2 e^2}{6\rho}, \quad (2)$$

where $B_m$ is the maximum induction, $e$ is the thickness of the sheet, $f$ the frequency, and $\rho$ the resistivity.

$P_h$ is the area of the hysteresis curve in the quasi-static mode times the frequency $f$

$$P_h = f \oint B \, dH. \quad (3)$$

The component $P_a$ is obtained through Eq. (1), according to the formula $P_a = P_t - P_{cl} - P_h$. The $P_{cl}$ component is calculated with Eq. (2), while $P_t$ and $P_h$ are experimentally determined.

### 3.2. Loss separation applied to study the effect of grain size

In Fig. 1, what is noteworthy is the high $P_a$ for the sample with $G_s = 13\,\mu$m. This should be attributed to an effect of the thickness on $P_a$. The classical eddy loss changes as a function of grain size in Fig. 1, but this is a consequence of the different skin-passes (implying different thicknesses $e$, when using Eq. (2))

Fig. 1 also shows that higher losses are systematically found for the transverse direction, and further that this effect is due to systematic increase in the hysteresis loss component. Measurements of crystallographic texture (see Fig. 2) showed the presence of the Goss texture component (1 1 0) [0 0 1], and this explains the anisotropy of the

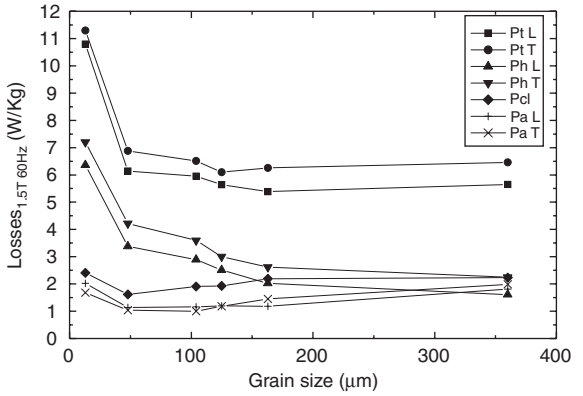


Fig. 1. Effect of grain size in the different losses components $P_t$, $P_h$, $P_a$, and $P_{cl}$, in the transverse ($T$) and longitudinal ($L$) directions.

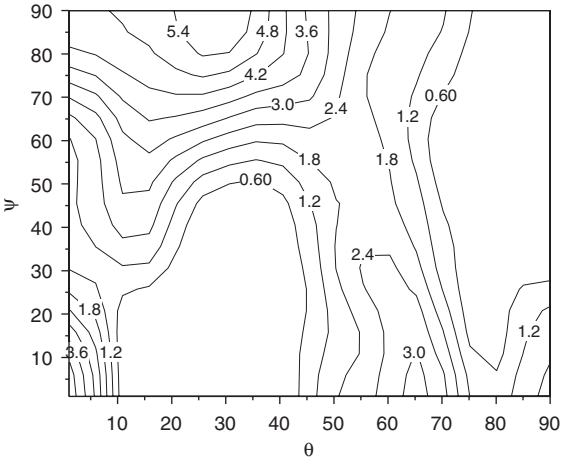


Fig. 2. Texture of the sample with 17% reduction, after recrystallization (grain size 48 μm). ODF, section $\Phi = 45^\circ$. Roe notation.

magnetic properties [10,11]. The Goss orientation (1 1 0) [0 0 1] is a typical recrystallization texture component in steels [12–14].

It is also observed (Fig. 3) that the optimum grain size changes as a function of frequency. The optimum grain size tends to increase when the frequency is decreased. This result will be used for testing the model for estimation of the optimum grain size for minimizing losses.

The effect of the grain size on the losses is one of the strongest arguments for the existence of a physical basis for the loss separation procedure,

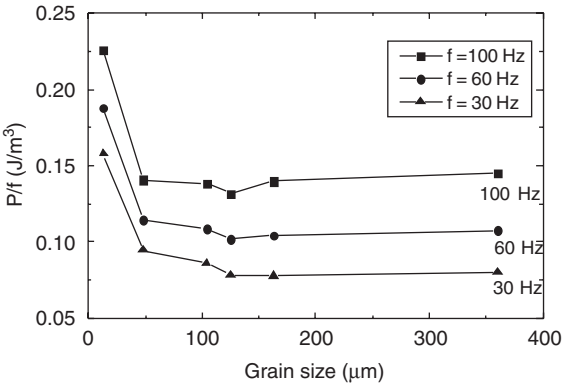


Fig. 3. Change of the optimum grain size to reduce losses when frequency is modified. The losses per cycle ($P/f$) are shown for the transverse direction.

because two different trends—on $P_h$ and on $P_a$—are clearly observed.

### 3.3. A model to predict the optimum grain size to minimize the iron losses

Loss separation enables the prediction of the optimum grain size. To get this estimate, it is only necessary to solve two problems: writing $P_h$ as function of grain size, i.e. $P_h(G_s)$ and, in analogous way, writing $P_a(G_s)$.

#### 3.3.1. $P_h$ as function of grain size

A simple reasoning can explain the dependence of the coercive force (or the hysteresis component $P_h$) on the inverse of grain size ($1/G_s$), as experimentally observed. It has been admitted [15–18] that formation and annihilation of domain walls originate energy dissipation, that is, losses. Thus, the only necessary hypothesis is the assumption that the hysteresis losses are directly proportional to the area of domain walls created and annihilated during the process of magnetization reversal. In the case of a cubic grain with volume $G_s^3$, the area of domain wall created will be proportional to $G_s^2$. Thus, the energy spent per unit volume will be proportional to $1/G_s$. This is in accordance with the experimental law $1/G_s$ earlier found by Yensen and Ziegler [19]. Thus, the coercivity and the quasi-static energy losses $E_{qs}$

(where $E_{qs} = P_h/f$) can be written as a constant plus another term proportional to $1/G_s$.

### 3.3.2. $P_a$ as function of grain size

The next step is obtaining an expression for $P_a$ ($G_s$). From the analysis of several published experimental data [3–5] we find an empirical relationship indicating $P_a \propto G_s^{1/2}$. There is a theoretical justification for this dependence. During the 1950s, several studies [20–22] introduced the effect of existence of domain walls into the Maxwell equations used to find the Eq. (2). All those models [20–22] predicted that $P_a$ would increase proportionally to $D/e$, where $D$ is the equilibrium distance between domain walls. Eq. (4) is the result found for the "Pry and Bean model" [22]:

$$P_a = (\eta - 1)P_{cl},$$
$$\text{with the non-dimensional } \eta \cong 1.63(D/e). \tag{4}$$

The domain size changes continuously through a hysteresis cycle—a function of the induction $B$. This makes very difficult to produce a rigorous theoretical model, which would take into account the whole microstructure and also the changing domain configuration. However, we will be satisfied if we obtain as an approximation a simple, but useful, model. In this simplified model, all the further discussion in this section refers to the demagnetized state. We assume that the demagnetized state can be considered as representative of the whole hysteresis cycle, especially if the magnetic induction $B$ is far from the saturation.

The average equilibrium distance between domain walls, $D$, can easily be estimated [23,24]. The following example described in Eqs. (5) and (6) is for a demagnetized sample, in the quasi-static regime. The sum, $E_t$, of the magnetostatic energy and of the domain wall energy ($\gamma$) per unity volume is given by (in the case of cubic grains):

$$E_t = \frac{\beta D \mu_0 M_s^2}{G_s} + \frac{\gamma}{D}, \tag{5}$$

where $M_s$ is the saturation magnetization, $\beta$ is a non-dimensional constant, whose value depends on the domain wall configuration [24]. Minimizing $E_t$ (making $dE_t/dD = 0$) we obtain

$$D = \sqrt{\frac{\gamma G_s}{\beta \mu_0 M_s^2}}. \tag{6}$$

Eq. (6) indicates that $D$ is proportional to $G_s^{1/2}$. This equation was deduced for the demagnetized condition, in the quasi-static regime. Haller and Kramer [15,16] have shown that, for a dynamic condition, the number of domain walls continuously increases with frequency. We can assume that, even in dynamic conditions, $D$ is proportional to $G_s^{1/2}$.

For the effect of frequency $f$ on the losses, $P_a \propto f^{3/2}$ is assumed (this information can also be considered empirical). As mentioned above, it can be experimentally determined that the number of domain walls increases with the square root of frequency [15,16,25]. Those determinations indicate [25] that $D \propto 1/f^{1/2}$ for the frequency range between $10^0$ and $10^3$ Hz. If this is substituted in Eq. (4), the experimental relationship $P_a \propto f^{3/2}$ is also found, when $\eta \gg 1$.

### 3.3.3. The optimum grain size

From the relationships discussed in the Section 3.3.2, we get now the following approximate equation for the anomalous losses $P_a$:

$$P_a = c_1 G_s^{1/2} \frac{1}{\rho} e^2 B_{max}^2 f^{3/2}, \tag{7}$$

where $c_1$ is a constant to be experimentally determined.

Eq. (7) is in agreement with the empirical observations [4,5] that indicate $P_a \propto G_s^{1/2}$.

The equation for $P_h$ is (following also Steinmetz law [26]):

$$P_h = \left(c_2 + \frac{c_3}{G_s}\right) B_{max}^q f, \tag{8}$$

where $c_2$ and $c_3$ are constants to be experimentally determined.

Adding Eqs. (7) and (8) to obtain $P_t$ and making $dP_t/dG_s = 0$, the optimum grain size $G_{sOp}$ for minimizing the losses is found

$$G_{sOp} = \left(\frac{c_4 \rho}{B^{2-q} e^2 f^{1/2}}\right)^{2/3}, \tag{9}$$

where $c_4$ is also a constant to be experimentally determined. The optimum grain size dependence with thickness needs further clarification, as Eq. (4) was developed for grain oriented steels, where the grains occupy the whole thickness. This is not the case in non-oriented steels.

Steinmetz [26] obtained experimentally at the end of the XIX Century that $q = 1.6$. It leads to $G_{sOp} \propto B^{-0.27}$, that is, $G_{sOp}$ is not much affected by the magnetic induction. Emura and Landgraf [27] confirmed $q = 1.6$, but only up to 1.2 T. From 1.2 to 1.5 T $q$ increases [27], so the effect of $B$ on $G_{sOp}$ is even smaller.

Eq. (9) indicates that $G_{sOp}$ increases with the resistivity. This is in agreement with the experimental data of Shimanaka et al. [2], that found that the optimum grain size increases when the Silicon—that is an alloying element that increases resistivity—content increases.

### 3.4. Application of the model

Eq. (9) should be tested with experimental results like those of Figs. 1 and 3. However, in that group of results there is also an effect of thickness of the sheet (see Fig. 1), that should increase $P_a$. For the test of the model the thickness will be fixed. All previous equations presented losses in W/m$^3$. To adjust them to the more usual W/kg, the effect of material density has to be included. The point $G_s = 163\,\mu m$ (thickness $e = 0.51$ mm) will be used as reference. For this point, $P_a = 1.45$ W/kg. The example is for the transverse direction of the sheets.

By means of the least-squares method the equation $P_h = 2.52 + 62.5\ (1/G_s)$ was found, for 60 Hz, with $G_s$ given by μm and $P_h$ by W/kg. The classical losses $P_{cl}$ was estimated with ($e = 0.51$ mm, $\rho = 20.5\,\mu\Omega$ cm, $B = 1.5$ T, $f = 60$ Hz), resulting in $P_{cl} = 2.15$ W/kg. These values were used for the construction of Fig. 4.

It should be remembered that the model used in Fig. 4 is not directly comparable with the experimental results of Fig. 1 because the effects of thickness on the losses.

For the adopted experimental conditions—that include the chemical composition of the steel—the model showed in Fig. 4 predicts a minimum at 110 μm. Taking into account the uncertainty of the experimental results (for example, the uncertainty of grain size measurement is 10%), it is in good agreement with the experimental results (see Fig. 3).

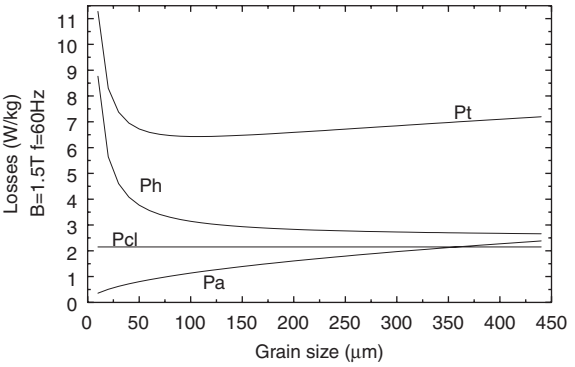


Fig. 4. Result of application of the model described in Section 3.3. Effect of the grain size the different losses components $P_t$, $P_h$, $P_a$, and $P_{cl}$. Transverse direction.

The model (Eq. (9)), predicts $G_{sOp1} = G_{sOp2}\,(f_2/f_1)^{1/3}$. If we chose $f = 30$ and 100 Hz, $G_{sOp(100\,Hz)} = 0.67\ G_{sOp(30\,Hz)}$ is obtained. If the values from Fig. 3 for $G_{sOp}$ 100 and 30 Hz are used—respectively 125 and 163 μm—the ratio 125/163 results 0.76, that should be compared to the theoretical 0.67, a very good agreement.

## 4. Conclusions

A model able to predict the optimum grain size for electrical steels—used either in motors or transformers—is presented.

The model predicts that the optimum grain size decreases if: resistivity decreases or frequency increases or thickness of steel sheet increases.

It is very important to note that the optimum grain size is a function of the frequency. Thus, for *each working situation* (e.g. each working frequency), there will be a new choice of material.

The model can be used either by steel producers for improvement of the steel loss characteristics or by motor producers for choosing a material when designing electrical motors.

## Acknowledgments

MF de Campos would like to acknowledge the support from CAPES (Programa ProDoc) and FAPESP proc. 01/09122-4. The authors acknowledge CNPq, proc. 504762/2004-4.

## References

[1] F.E. Werner, R.I. Jaffee, J. Mat. Eng. Perf. 1 (1992) 227.
[2] H. Shimanaka, Y. Ito, K. Matsumura, B. Fukuda, J. Magn. Magn. Mat. 26 (1982) 57.
[3] M.F. Littmann, IEEE Trans. Magn. MAG-7 (1971) 48.
[4] K. Matsumura, B. Fukuda, IEEE Trans. Magn. MAG-20 (1984) 1533.
[5] M. Shiozaki, Y. Kurosaki, J. Mat. Eng. 11 (1989) 37.
[6] F.J.G. Landgraf, J.C. Teixeira, M. Emura, M.F. de Campos, C.S. Muranaka, Mater. Sci. Forum 302–303 (1999) 440.
[7] F.J.G. Landgraf, M. Emura, J.C. Teixeira, M.F. de Campos, C.S. Muranaka, J. Magn. Magn. Mat. 196–197 (1999) 380.
[8] R. Boll, Weichmagnetische Werkstoffe. Vacuumschmelze, Hanau, Germany, 1990 (in German).
[9] J.J. Thomson, Electrician 28 (1892) 599.
[10] M. Emura, M.F. de Campos, F.J.G. Landgraf, J.C. Teixeira, J. Magn. Magn. Mat. 226–230 (2001) 1524.
[11] M.F. de Campos, F.J.G. Landgraf, A.P. Tschiptschin, J. Magn. Magn. Mat. 226–230 (2001) 1536.
[12] R.K. Ray, J.J. Jonas, R.E. Hook, Int. Mat. Rev. 39 (4) (1994) 129.
[13] M.F. de Campos, F.J.G. Landgraf, R. Takanohashi, F.C. Chagas, I.G.S. Falleiros, G.C. Fronzaglia, H. Khan, ISIJ Int. 44 (2004) 591.
[14] M.F. de Campos, F.J.G. Landgraf, I.G.S. Falleiros, G.C. Fronzaglia, H. Khan, ISIJ Int. 44 (2004) 1733.
[15] T.R. Haller, J.J. Kramer, J. Appl. Phys. 41 (1970) 1034.
[16] T.R. Haller, J.J. Kramer, J. Appl. Phys. 41 (1970) 1036.
[17] M. Guyot, A. Globus, Phys. Stat. Sol. (b) 59 (1973) 447.
[18] M. Guyot, V. Cagan, J. Magn. Magn. Mat. 101 (1991) 256.
[19] T.D. Yensen, N.A. Ziegler, Trans. ASM 23 (1935) 536.
[20] H.J. Williams, W. Shockley, C. Kittel, Phys. Rev. 80 (1950) 1090.
[21] E.W. Lee, Proc. IEE 105C (1958) 337.
[22] R.H. Pry, C.P. Bean, J. Appl. Phys. 29 (1958) 532.
[23] C. Kittel, Rev. Mod. Phys. 21 (1949) 541.
[24] J.W. Shilling, G.L. Houze Jr., IEEE Trans. Magn. MAG-10 (1974) 195.
[25] Y. Sakaki, IEEE Trans. Magn. MAG-16 (1980) 569.
[26] C.P. Steinmetz, Trans. AIEE 9 (1892) 3.
[27] M. Emura, F.J.G. Landgraf, unpublished.